Modeling and Simulation of an Isothermal CO_2 Capture System using a Hollow Fiber Membrane Contactor

Wanderson F. A. dos Passos[1], Arioston A. de Morais Jr[1]

[1]*Dept. of Chemical Engineering, Federal University of Paraíba*
Campus I – Lot. Cidade Universitária, 58051-900, João Pessoa - PB, Brazil
Wanderson_f000@outloook.com, aamj@ct.ufpb.br

Abstract. This manuscript provides an analyzes of a one-dimensional modeling approach for post-combustion CO2 capture in a Hollow Fiber Membrane Contactor (HFMC), which uses a 30% (w/w) MEA (monoethanolamine) solution as a solvent. A reactive absorption is considered, with variable gas and liquid resistances. The influence of the volumetric rate ($G°$) on the system parameters was evaluated, and then, the system behavior was studied, fixing the parameters to achieve a capture ratio of 90%. The MATLAB 2021a® software was used to solve the equations, and a routine was created, allowing to solve the problem as an initial value problem (IVP), which shown to be efficient.

Keywords: modeling, carbon dioxide capture, hollow fiber membrane contactor, reactive absorption.

1 Introduction

Due its influence on the global warming and for being one of the greenhouse gases, carbon dioxide (CO_2) called the attention of the global researchers around the world. Thus, the so-called Carbon Capture and Storage (CCS) has been studied along the last decades [1, 2].

Despite the conventional methods for post-combustion CO_2 capture are considered to be the bests available ways [2], membrane-based methods have gained prominence due to their distinct advantages [3]. Gabelman et al. [4] and Rivero et al. [3] explain important aspects about the operability and modeling of the Hollow Fiber Membrane Contactor (HFMC). The HFMC will be the object of study of this manuscript.

2 Methodology

The HFMC consists in a shell which is packed with hydrophobic microporous tubes (hollow selective cylindric fibers) where only the CO_2 can pass through. This process occurs by physical absorption and chemical reaction in at least three steps: the CO_2 is transferred from the gas bulk to the gas film (the gas boundary layer formed right at the mouth of the micropores), then diffused through the pores of the membrane, and finally absorbed by the solvent (amine solution) where the reaction happens [5–7].

2.1 System characteristics

The size of the system considered on this manuscript is in pilot scale, and the geometric parameters are between the range of the commercialized HFMCs: high fiber volume fractions ($\varphi \geq 5$) and small fiber external radii ($r_e \leq 10^3$ m) [8]. A number of tubes of 24000 was considered, and for a given fiber volume fraction (φ), external radius (r_e), a relative thickness of the fiber (δ/r_e, where δ stands for the thickness) and a fixed ratio of the liquid velocity and inlet gas velocity (u_L/u_G^0) [8], the shell radio (r_s) can be estimated. A circular internal section of the membranes is considered, and the equivalent hydraulic diameter (d_h) was considered to represent the geometry of the external flow section [8, 9].

The range of the volumetric rate of the post-combusted gas on the inlet side (G^0) studied is $[0 - 1] \times 10^{-1}$ m³/s, which have an initial molar fraction of CO_2 (y_A^0) of 0.15, and the liquid rate (L) is estimated from the

velocities ratio.

The solvent (liquid phase) consists in an aqueous monoethanolamine (MEA) solution 30% (w/w), widely used in the CO_2 absorption industry and researches [10–14], and it's is considered flowing at the lumen side of the fiber, whereas the gas mixture flows at the external side of the membrane. Both of them leak in a counter-current flow, and a laminar velocity profile is considered for them.

2.2 Model assumptions

Important model assumptions are summarized below (based on considerations of Rode et al. [8] and Zaidiza et al. [5]).

Remark 1: Phases. The gas phase consists in a mixture of CO_2 (which is the solute) and saturated air (H_2O + N_2 + O_2), and its overall volumetric flow varies in an ideally behavior with the gas pressure. The liquid phase is an aqueous solution of MEA (as said before), and its volumetric flow remains constant because no pressure drop on the liquid phase is considered.

Remark 2: System. The system is at steady state and varies only with the axial coordinate (consisting in a unidimensional model, neglecting the radial and angular variations). The gas flows surrounding the fibers (shell side), in a counter-current configuration related to the liquid (which flows inside the membrane).

Remark 3: Membranes. A non-wetted model for the membranes (reducing the mass transfer resistance [15]) is considered in this paper, which means that all porous membranes are hydrophobics and the gas-liquid interface is always located at the internal surface of the membranes. The pore size is uniform throughout the membrane.

Remark 4: Equilibrium. The Henry's Law is used to describe the equilibrium at the gas-liquid interface. The Henry constant is considered unvarying due the concentration range used (so the volumetric gas-liquid partition coefficient m) [16].

Remark 5: Temperature and properties. The isothermal conditions area assumed, so the temperature remains constant at the entire process. Liquid properties (such as density and viscosity) remain constant too.

2.3 Mass transfer, chemical reaction

The concept of resistances in series was used to model the mass transfer in the process, by estimating a local overall resistance (then an overall mass transfer coefficient K_{OV}) [4, 5], using the local mas transfer coefficients at the gas film, liquid film and the membrane pores. The two-film theory was applied to describe the transfer at the gas-liquid interface, adding the chemical reaction on the liquid side [17].

For a given fluid F leaking with a laminar flow in a cylindrical pipe, the local mass transfer coefficient can be estimated using the dimensionless Graetz number (Gz_F), using the hydraulic diameter at the flow section. This analogy is commonly used in HFMCs for the flow inside the fibers [18, 19], but Rode [8] shows that applying this analogy to an array of cylinders is also suitable, considering a fully developed profile for both the gas-side and liquid-side. The Graetz number is given by eq. (1):

$$Gz_F = \frac{D_{A,F} z}{v_F d_h^2} \tag{1}$$

where F can be either the gas or liquid phase (represent by G and L subscription, respectively), $D_{A,F}$ is the diffusion coefficient of CO_2 on the fluid, z is the axial coordinate, v_F is the interstitial velocity given by the ratio between the superficial velocity of the fluid (u_F) and the specific flow section external (ε_{ext}, surround the fibers) or internal (ε_{int}, at the lumen side), given by the ratio of the flow section and the overall reactor section, and d_h is the hydraulic diameter, which also depend on the fiber side of the flow and it is given by eqns. (2) and (3):

$$d_{h,ext} = 2r_e\,(1-\varphi)/\varphi \tag{2}$$

$$d_{h,int} = 2r_e(1-\delta/r_e). \tag{3}$$

Known the Graetz number, the Sherwood number can be estimated (so the local mass transfer coefficient et the gas and liquid sides) [5-8] by the following equations:

$$Gz_F < 0.03 \rightarrow Sh_F = 1.3Gz_F^{-1/3} \tag{4}$$

$$Gz_F > 0.03 \rightarrow Sh_F = 4.36 \tag{5}$$

$$Sh_F = \frac{k_F d_h}{D_{j,F}} \tag{6}$$

where k_F is the mass transfer coefficient which can be used for the gas (k_G) or for the liquid (k_L).

The mass transfer through the membrane is leaded by the diffusion, and the mass transfer coefficient of the membrane (k_M) can be calculated by eq. (7) using a Fick diffusion mechanism [9], which is already discussed on the literature being suitable for this process [4, 8]:

$$k_M = \frac{D_{A,G}}{\delta}\left(\frac{\varepsilon}{\tau}\right) \tag{7}$$

where ε/τ stands for the membrane permeability.

The overall mass transfer coefficient can now be calculated using the eq. (8):

$$\frac{1}{K_{OV}} = \frac{1}{mEk_L} + \frac{1-\delta/r_e}{\delta/r_e}\ln\left(\frac{1}{1-\delta/r_e}\right)\frac{1}{k_M} + \frac{1-\delta/r_e}{k_G} \tag{8}$$

where m can be calculated by the inverse of the dimensionless Henry's constant and E stands for the enhancement factor, which decrease the liquid film resistance due the chemical reaction [17].

It was considered that the chemical reaction occurs at the liquid side boundary layer, with irreversible, bimolecular and second-order characteristics [5, 8]. The mathematical expression used for the reaction is represented for the eq. (9), where A stands for the CO_2 and B for the MEA solution:

$$2B_{(l)} + A_{(g)} \rightarrow B_2A_{(l)}. \tag{9}$$

To describe the reaction regime, two dimensionless number were used: the Hatta number (Ha) and the limiting (or asymptotic) enhancement factor (E_{lim}) [8, 20]. Three regimes should be considered to calculate the enhancement factor, as represented by eqns. (10) – (12) [5, 8]:

$$\frac{E_{lim}}{Ha} > 50 \rightarrow E = \sqrt{1+Ha^2} \tag{10}$$

where the process is not limited by the MEA diffusion,

$$\frac{E_{lim}}{Ha} < 0.02 \rightarrow E = E_{lim} \tag{11}$$

where there is limitation by the MEA diffusion,

$$0.02 < \frac{E_{lim}}{Ha} < 50 \rightarrow E = \frac{Ha\sqrt{\frac{(E_{lim}-E)}{(E_{lim}-1)}}}{\tanh\left[Ha\sqrt{\frac{(E_{lim}-E)}{(E_{lim}-1)}}\right]} \tag{12}$$

which is an intermediate situation.

The Hatta number and the limiting enhancement factor can be calculated by eqns. (13) and (14):

$$Ha = \frac{\sqrt{D_{A,L}k_r C_{B,L}}}{k_L} \tag{13}$$

$$E_{lim} = 1 + \frac{C_{B,L}D_{B,L}}{2mC_{A,G}D_{A,L}} \tag{14}$$

where k_r is the kinetic constant and $C_{B,L}$ and $C_{A,G}$ are the concentration of MEA in the liquid and CO_2 in the gas, respectively.

The kinetic can be described by its expression on eq. (15) (which gives the reaction rate r_A in $mol_A m_L^{-3} s^{-1}$):

$$r_A = -k_r C_{A,L} C_{B,L} \tag{15}$$

where $C_{A,L}$ and $C_{B,L}$ are the concentrations of CO_2 and MEA in the liquid phase, and the kinetic constant (in $m_L^3 mol_A^{-1} s^{-1}$) is computed by eq. (16):

$$k_r = 4.4 \times 10^8 \exp\left(-\frac{5400}{T}\right) \tag{16}$$

where T is the temperature of the process.

To see the behavior of CO_2 on in the transfer process, its molar fraction on the gas-phase (y_A), the capture ratio (θ) [8] and the local absorbed flux Φ_A (in mol s^{-1} m^{-3}) were used. The CO_2 molar fraction was calculated by eq. (17):

$$y_A = C_{A,G}\frac{RT}{P_G} \tag{17}$$

where $C_{A,G}$ and P_G stand for the concentration of CO_2 and the pressure, respectively, on the gas-phase, the capture ratio was estimated by eq. (18):

$$\theta = 1 - \frac{(1-y_A^0)y_A}{(1-y_A)y_A^0} \tag{18}$$

and the absorbed local flux was computed by eq. (19):

$$\Phi_A = a_{int}K_{OV}C_{A,G} \tag{19}$$

where a_{int} stands for the internal specific interfacial area and is given by eq. (20):

$$a_{int} = 2\varphi(1-\delta/r_e)/r_e. \tag{20}$$

2.4 Balance equations

The differential equation system is formed by three balances: a CO_2 molar balance, a MEA molar balance and a gas momentum balance. A dimensionless system is described by Rode et al [8] and Zaidiza et al [5], however this paper shows the non-dimensionless system adapted from the proposal of Rode.

Remark 1: CO_2 differential molar balance. Considering the CO_2 concentration in the gas varying with the transfer and its pressure, the molar balance results in the eq. (21):

$$\frac{dC_{A,G}}{dz} = \frac{C_{A,G}}{P_G}\left[\frac{dP_G}{dz} - \frac{a_{int}K_{OV}P_G^0}{u_G^0(1-y_A^0)}\left(\frac{P_G}{P_G^0} - \frac{C_{A,G}}{C_{A,G}^0}y_A^0\right)^2\right] \tag{21}$$

where P_G^0 is the inlet gas pressure and $C_{A,G}^0$ stands for the inlet concentration of CO_2.

Remark 2: MEA differential molar balance. Considering a counter-current arrangement and the reaction stoichiometry, the MEA balance in the liquid phase results in the eq. (22):

$$\frac{dC_{B,L}}{dz} = \frac{2a_{int}K_{OV}C_{A,G}}{u_L} \tag{22}$$

which should be negative if a concurrent flow is applied.

Remark 3: Gas momentum balance. The pressure drop at the shell side of the HFMC can be described by a Kozeny-type equation [5, 8, 21] given by eq. (23), with a Kozeny constant fitted to a fiber-bundle geometry:

$$\frac{dP_G}{dz} = -a_{int}\left[\frac{2\kappa\mu_G\varphi}{r_e(1-\varphi)^3\left(1-\frac{\delta}{r_e}\right)}\right]\frac{u_G^0(1-y_A^0)}{\left(\frac{P_G}{P_G^0} - \frac{C_{A,G}}{C_{A,G}^0}y_A^0\right)} \tag{23}$$

where μ_G is the viscosity of the gas-phase and κ stands for the Kozeny constant, which is given by eq. (24) for a range of $0.3 < \varphi < 0.6$:

$$\kappa = 5.50\varphi^2 - 7.87\varphi + 7.73. \tag{24}$$

3 Results and discussion

Due the counter-current configuration of the system, the model forms a boundary value problem (BVP), as the concentration of free MEA at $z = 0$ ($C_{B,L}^{0}$) is not known (it is known only the concentration in Z, which is the HFMC length and the inlet side of liquid). Nevertheless, the system was solved as an initial value problem (IVP) using the *ode45* routine from Matlab R2021a® with and initial guess of $C_{B,L}^{0}$, and a little routine was created to fix that estimative. The free MEA concentration at Z is considered to have CO_2 loading (α^{Z}) of 0.484, so that routine solved the loading of CO_2 at the initial point (α^{0}).

3.1 Simulation conditions

At least two analyses with different simulation conditions were done: a sensitive analysis for the influence of the volumetric rate of the gas-phase on the capture ratio, CO_2 concentration on the gas, consumed MEA and pressure drop (where Z was fixed in 2 m and G^{0} varies from 0 to 1×10^{-1} m³/s), and an analysis of the behavior of the process with the axial coordinate z (fixing $G^{0} = 1.5 \times 10^{-4}$ m³/s and $Z = 1.141$ m to achieve a capture ratio of 90%).The parameters used for the simulations are shown on Tab. 1 [11, 22–27]:

Table 1. Simulation parameters

Parameter	Nomenclature	Value	Units
Fiber volume fraction	φ	0.6	dimensionless
External fiber radius	r_e	1×10^{-3}	m
Relative membrane thickness	δ/r_e	0.4	dimensionless
Membrane permeability	ε/τ	0.12	dimensionless
Number of fibers	N_t	24000	dimensionless
Temperature	T	313	K
Inlet gas pressure	P_G^0	1.05×10^{5}	Pa
Inlet superficial velocity ratio	u_L/u_G^0	4.79×10^{-3}	dimensionless
Inlet molar fraction of CO_2	y_A^0	0.15	dimensionless
Inlet molar concentration of CO_2	$C_{A,G}^0$	6.0524	mol_A/m^3
Gas viscosity	μ_G	1.5×10^{-5}	Pa s
Diffusion coefficient of CO_2 on gas	$D_{A,G}$	1.65×10^{-5}	m^2/s
Inlet solvent concentration of free MEA	$C_{B,L}^Z$	2544	mol_B/m^3
Diffusion coefficient of CO_2 on liquid	$D_{A,L}$	1.29×10^{-9}	m^2/s
Diffusion coefficient of MEA on liquid	$D_{B,L}$	1.04×10^{-9}	m^2/s
Volumetric gas-liquid partition coefficient	m	0.610	m_G^3/m_L^3

3.2 Volumetric rate influence

As said, the configuration of the HFMC was fixed and the volumetric flow was variated. Figure 1 shows the stationary behavior of the process at the variation.

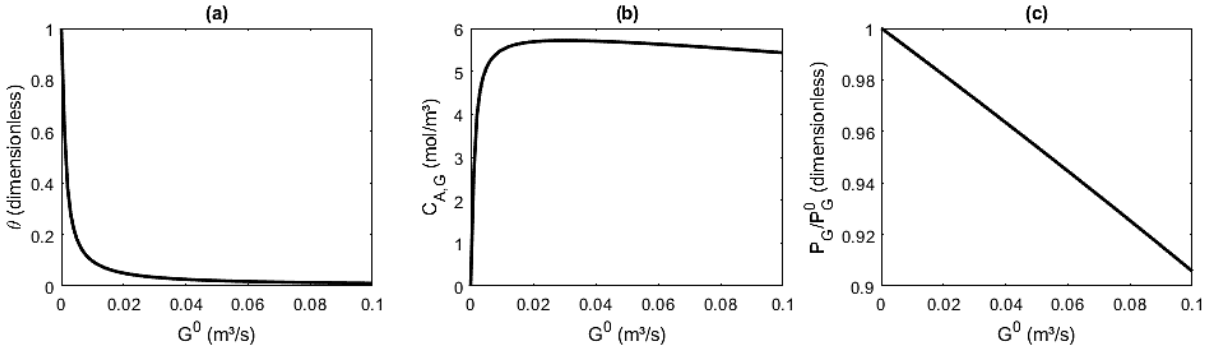

Figure 1. Sensitivity analysis for the inlet gas volumetric rate

As seen on part (a) of Fig. 1, the decrease of capture ratio is steep when increasing the inlet gas volumetric rate, until a sharp curve and start to decrease smoothly (when the pressure drop starts getting significant influence, as seen on part (c), and the CO_2 concentration starts to decrease due the volume increasing).

For the fixed configuration (in pilot-scale), only low volumetric rates ($G^0 < 5.6 \times 10^{-4}$) are allowed if capture ratios greater than 80% are required (as shown on Fig. 2).

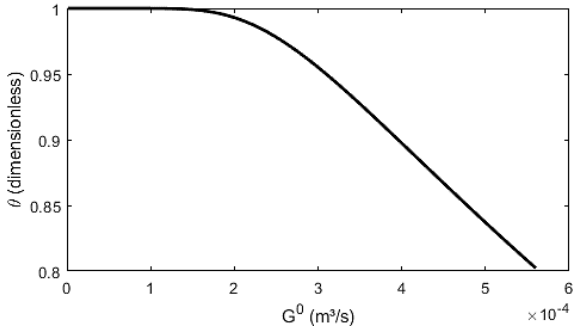

Figure 2. Sensitivity analysis for the inlet gas volumetric rate for $\theta > 80\%$

3.3 Behavior of HFMC with axial coordinate

Figure 3 shows the process behavior with the dimensionless axial coordinate (z/Z), where Z was fixed accordingly to the capture ratio ($Z = 1.141$ m to $\theta = 0.90$), using a volumetric ration of 1.5×10^{-4}.

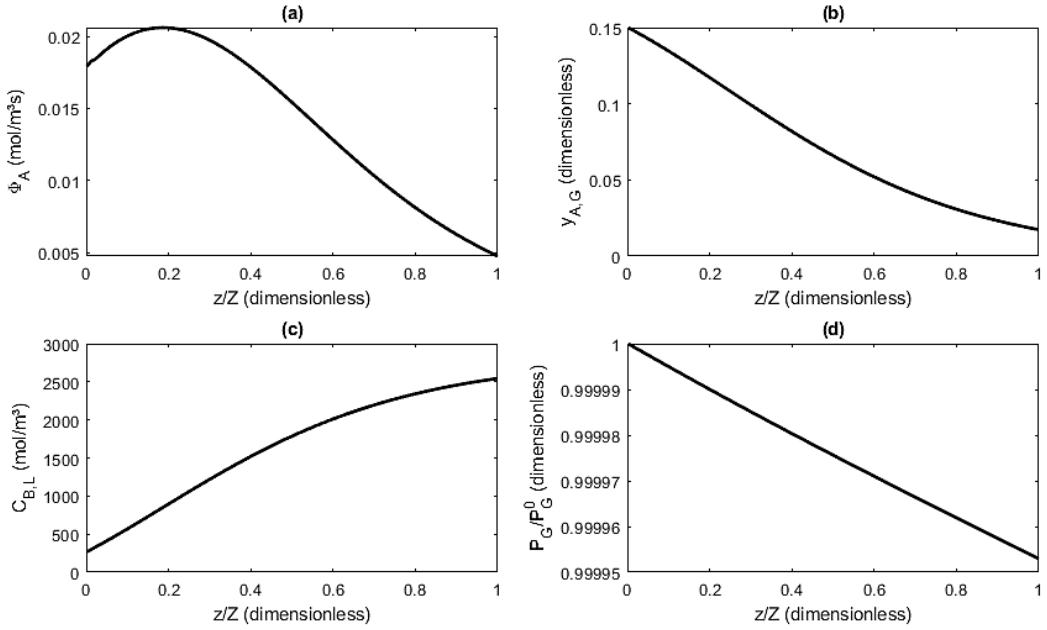

Figure 3. Solution of the system for a capture ratio of 90%

The variation of the flux (part (a) of Fig. 3) shows that near the $z/Z = 2$ point, the flux of CO_2 is maximum, then starts to decrease due the behavior of CO_2 concentration on the gas. The CO_2 molar fraction (part (b)) starts to decrease from 0.15 until gets the value for the required capture ratio ($y_A^Z = 0.0173$). The part (c) shows that the created routine fits very well to fix the initial value of $C_{B,L}^0$. The pressure drop on the gas-phase is neglectable, as shown on part (d). So, for this system, the configuration of the HFMC is fully applicable.

4 Conclusions

This manuscript aimed to develop a modeling and simulation for CO2 capture using a hollow fiber membrane

contactor (HFMC) and evaluate the behavior of the process through important changes in design variables. The model tested was a little different from the model taken from the literature (non-dimensionless), but it gets good results as expected. Was observed that, increasing the inlet gas flow (G°), the capture ratio (θ) decreases fast, allowing only low rates depending on the scale of interest. The way to solve the problem proved to be very effective, as it was accompanied to a routine to fix the initial guess of the concentration of free MEA.

Authorship statement. The authors hereby confirm that they are the sole liable persons responsible for the authorship of this work, and that all material that has been herein included as part of the present paper is either the property (and authorship) of the authors, or has the permission of the owners to be included here.

References

[1] P. Bains, P. Psarras and J. Wilcox. "CO2 capture from the industry sector." *Progress in Energy and Combustion Science*, vol. 63, pp. 146–172, 2017.
[2] R. Steeneveldt, B. Berger, and T. A. Torp. "CO2 capture and storage: closing the knowing–doing gap." *Chemical Engineering Research and Design*, vol. 84, n. 9, pp. 739–763, 2006.
[3] J. R. Rivero, et al. "Hollow fiber membrane contactors for post-combustion carbon capture: A review of modeling approaches." *Membranes*, vol. 10, n. 12, p. 382, 2020.
[4] A. Gabelman and S. T. Hwang. "Hollow fiber membrane contactors". *Journal of Membrane Science*, vol. 159, n. 1–2, pp. 61–106, 1999.
[5] D. A. Zaidiza, et al. "Modeling of CO2 post-combustion capture using membrane contactors, comparison between one- and two-dimensional approaches". *Journal of membrane science*, vol. 455, pp. 64–74, 2014.
[6] D. A. Zaidiza, et al. "Adiabatic modelling of CO2 capture by amine solvents using membrane contactors". *Journal of membrane science*, vol. 493, pp. 106–119, 2015.
[7] D. A. Zaidiza, et al. "Rigorous modelling of adiabatic multicomponent CO2 post-combustion capture using hollow fibre membrane contactors". *Chemical Engineering Science*, vol. 145, po. 45–58, 2016.
[8] S. Rode et al. "Evaluating the intensification potential of membrane contactors for gas absorption in a chemical solvent: A generic one-dimensional methodology and its application to CO2 absorption in monoethanolamine". *Journal of membrane science*, vol. 389, pp. 1–16, 2012.
[9] R. Prasad and K. K. Sirkar. "Dispersion-free solvent extraction with microporous hollow-fiber modules". *AIChE journal*, vol. 34, n. 2, pp. 177–188, 1988.
[10] K. P. Shen and M. H. Li. "Solubility of carbon dioxide in aqueous mixtures of monoethanolamine with methyldiethanolamine". *Journal of chemical and Engineering Data*, vol. 37, n. 1, pp. 96–100, 1992.
[11] F. A. Tobiesen, H. F. Svendsen and O. Juliussen. "Experimental validation of a rigorous absorber model for CO2 postcombustion capture". *AIChE journal*, vol. 53, n. 4, pp. 846–865, 2007.
[12] G. T. Rochelle. "Amine scrubbing for CO2 capture". *Science*, vol. 325, n. 5948, pp. 1652–1654, 2009.
[13] E. Gjernes et al. "Results from 30 wt% MEA performance testing at the CO2 Technology Centre Mongstad". *Energy Procedia*, vol. 114, pp. 1146–1157, 2017.
[14] A. Gladis et al. "Pilot scale absorption experiments with carbonic anhydrase-enhanced MDEA-Benchmarking with 30 wt% MEA". *International Journal of Greenhouse Gas Control*, vol. 82, pp. 69–85, 2019.
[15] R. Wang et al. "Influence of membrane wetting on CO2 capture in microporous hollow fiber membrane contactors". *Separation and Purification Technology*, vol. 46, n. 1–2, pp. 33–40, 2005.
[16] S. Ma'mun et al. "Solubility of carbon dioxide in 30 mass% monoethanolamine and 50 mass% methyldiethanolamine solutions". *Journal of Chemical & Engineering Data*, vol. 50, n. 2, pp. 630–634, 2005.
[17] O. Levenspiel. *Chemical reaction engineering*. John Wiley & Sons, 1998.
[18] J. L. Li and B. H. Chen. "Review of CO2 absorption using chemical solvents in hollow fiber membrane contactors". *Separation and Purification Technology*, vol. 41, n. 2, pp. 109–122, 2005.
[19] S. Karoor and K. K. Sirkar. "Gas absorption studies in microporous hollow fiber membrane modules". *Industrial & engineering chemistry research*, vol. 32, n. 4, pp. 674–684, 1993.
[20] W. J. Beek, K. M. K. Muttzall and J.M. van Heuven. *Transport Phenomena*. 2nd ed., John Wiley & Sons, 1999.
[21] J. Happel. "Viscous flow relative to arrays of cylinders". *AIChE Journal*, vol. 5, n. 2, pp. 174–177, 1959.
[22] S. Ma'mun and H. F. Svendsen. "Solubility of N2O in aqueous monoethanolamine and 2-(2-Aminoethyl-amino) ethanol solutions from 298 to 343 K". *Energy Procedia*, vol. 1, n. 1, pp. 837–843, 2009.
[23] S. Cheng, A. Meisen and A. Chakma. "Predict amine solution properties accurately". *Hydrocarbon processing*, vol. 75, n. 2, 1996.
[24] J.P. Poling, B.E. Prausnitz and J.M. O'Connell. *The Properties of Gases in Liquids*. 5th ed., McGraw Hill, 2000.
[25] E. D. Snijder et al. "Diffusion coefficients of several aqueous alkanolamine solutions". *Journal of Chemical and Engineering Data*, vol. 38, n. 3, pp. 475–480, 1993.
[26] G. F. Versteeg et al. "On the kinetics between CO2 and alkanolamines both in aqueous and non-aqueous solutions. An overview". *Chemical Engineering Communications*, vol. 144, n. 1, pp. 113–158, 1996.
[27] G. F Versteeg and W. P. M. Van Swaaij. "Solubility and diffusivity of acid gases (CO2, N2O) in aqueous alkanolamine solutions". *Journal of Chemical and Engineering Data*, vol. 33, pp. 29–34, 1988.